The Estimation of Angular Misalignments for Ultra Short Baseline Navigation Systems. Part II: Experimental Results

Hsin-Hung Chen

(*Institute of Applied Marine Physics and Undersea Technology, National Sun Yat-sen University, Kaohsiung, Taiwan, ROC*)
(E-mail: hhchen@faculty.nsysu.edu.tw)

An algorithm of alignment calibration for Ultra Short Baseline (USBL) navigation systems was presented in the companion work (Part I). In this part (Part II) of the paper, this algorithm is tested on the sea trial data collected from USBL line surveys. In particular, the solutions to two practical problems referred to as heading deviation and cross-track error in the USBL line survey are presented. A field experiment running eight line surveys was conducted to collect USBL positioning data. The numerical results for the sea trial data demonstrated that the proposed algorithm could robustly and effectively estimate the alignment errors. Comparisons of the experimental result with the analytical prediction of roll misalignment estimation in Part I is drawn, showing good agreement. The experimental results also show that an inappropriate estimation of roll alignment error will significantly degrade the quality of estimations of heading and pitch alignment errors.

1. INTRODUCTION. A line survey scheme was proposed in the previous companion paper, Part I (Chen, 2013), for Ultra Short Baseline (USBL) misalignment calibration, which is the simplest method to be performed with respect to the manoeuvring of a vessel. An iterative algorithm that allows estimating angular misalignments between attitude sensors and USBL transceiver was presented in Part I (Chen, 2013). This algorithm is based on the positioning errors caused by heading, pitch and roll misalignments when running a line survey over the area above a seabed transponder. The performance of the characteristic based iterative algorithm has been investigated and validated by simulations. In this paper, the proposed algorithm is further tested with USBL observations from a sea trial. In addition, a sensitivity analysis

of roll alignment error estimation was investigated in Part I (Chen, 2013), and its validity will be tested in this paper by the use of the sea trial data.

The line survey approach developed in Part I is based on the assumption that the vessel is able to move along a desired straight course line and its heading can be kept in line with the reference course while collecting USBL observations. In reality, while conducting a line survey, the vessel may move off the course line or its heading may deviate from the course direction. The distance a vessel is off the desired path is commonly known as the cross-track error. Even for those vessels with navigation and guidance systems, numerous studies are still being carried out to further optimize their manoeuvring controllers for minimization of heading deviation and cross-track error (Skjetne et al., 2005; Gierusz et al., 2007; Moreira et al., 2007). Therefore, both corrections for heading deviation and cross-track error in USBL calibration are made in the present paper to obtain accurate estimates of angular misalignment. With the aid of heading deviation and cross-track error corrections, the vessel trajectory for USBL calibration is not limited to a straight line, as was assumed in Part I (Chen, 2013), but can be any arbitrary curve.

2. HEADING DEVIATION CORRECTION. Though a straight course is simple for a vessel to follow, heading can be difficult to maintain when environmental forces act on the hull in an unpredictable manner. The vessel's crew may adjust engine power or alter the rudder to offset the external forces so that the desired straight-line course can be maintained. The heading of the vessel, however, may deviate from the course direction. The estimation of heading alignment error in the proposed algorithm is based on the slope of the transponder trajectory observed from the USBL transceiver. When a line survey is conducted with heading deviation, the observed transponder trajectory will be distorted, thus biasing the estimate of heading alignment error. The correction for the effect of heading deviation on USBL observations has to be made before the estimation of alignment errors.

To correct for heading deviation in the USBL measurements, the reference course of the vessel must be given first. For a vessel track which may be straight or, more commonly, curved, it can be fitted to a straight line by the use of the least-squared error approach. The fitted line is taken as the reference course. We consider a USBL line survey as depicted in Figure 1, with the reference course (dashed line), the course direction θ, and the heading deviation $\Delta\theta$. Three coordinate systems, $O_a X_a Y_a Z_a$, $O_t X_t Y_t Z_t$, and $O_h X_h Y_h Z_h$, are employed for heading deviation correction. The $O_a X_a Y_a Z_a$ coordinate system is an earth-fixed East-North-UP (ENU) frame with its origin on the sea surface over the top of the seabed transponder. The $O_t X_t Y_t Z_t$ coordinate system is a body-fixed reference frame for the USBL transceiver. The frame $O_h X_h Y_h Z_h$ is defined as a right-handed system such that its origin O_h is coincident with the origin O_t, its Z_h-axis is coincident with the Z_t-axis, and its Y_h-axis is along the direction of the course. When conducting a USBL line survey with heading deviation $\Delta\theta$, the position vector of the transponder, $\mathbf{P}_t$, is measured from the transceiver in the $O_t X_t Y_t Z_t$ coordinate system. However, the position vector of the transponder, $\mathbf{P}_h$, with respect to the $O_h X_h Y_h Z_h$ coordinate system is desired for keeping the vessel's heading in line with the course direction throughout the line survey. The correction for heading deviation is therefore to transform the measured position vector $\mathbf{P}_t$ from the coordinate system $O_t X_t Y_t Z_t$ to $O_h X_h Y_h Z_h$. According to the geometric scheme in
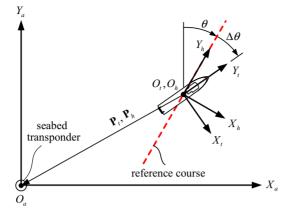
Figure 1. Vessel's heading deviates from the course direction while conducting a USBL line survey.

Figure 1, the position vector $\mathbf{P}_t$ can be transformed to the $O_h X_h Y_h Z_h$ coordinate system by the following computation of coordinate transformation:

$$\mathbf{P}_h = \begin{bmatrix} \cos \Delta\theta & \sin \Delta\theta & 0 \\ -\sin \Delta\theta & \cos \Delta\theta & 0 \\ 0 & 0 & 1 \end{bmatrix} \mathbf{P}_t \tag{1}$$

3. CROSS-TRACK ERROR CORRECTION. Environmental forces (wind, wave drift, current loads, etc.) can cause loss of the ability of a vessel to maintain a straight path on a predetermined course. When a vessel is off-course, the distance from the vessel to the course is defined as the cross-track error. The proposed algorithm for alignment error estimation is designed to follow the assumption that the vessel is able to move along a predefined straight course while performing USBL line survey. Therefore, if the vessel is off the desired course while running USBL survey, the USBL observations need to be corrected for cross-track error prior to the estimation of alignment errors.

In a manner similar to the correction for heading deviation described in Section 2, the correction for cross-track error begins with the linear regression of a vessel track. Figure 2 presents a solid curve showing the curved vessel track. The least-squared straight line fit through the vessel track represented by a dashed line in Figure 2 is taken as the reference course. In the absence of heading deviation, the Y_t-axis towards the direction of the reference course and the X_t-axis is perpendicular to the reference course. Given that, as shown in Figure 2, O_t is the position of the transceiver, the fitted straight line is heading in a direction of θ, and B is the intersection of the reference course and the X_t-axis. In terms of these, the cross-track error is the distance between points O_t and B. The correction for cross-track error can be achieved by relocating the vessel's position from point O_t to point B. Thus, the observed transponder position is changed from $\mathbf{P}_t$ to $\mathbf{P}_c$, as shown in Figure 2.

In the determination of the corrected transponder position $\mathbf{P}_c$, the coordinates of point B need to be known first. With respect to the global frame, say $O_a X_a Y_a Z_a$, let the equation of the reference course on the $X_a Y_a$ plane be given by

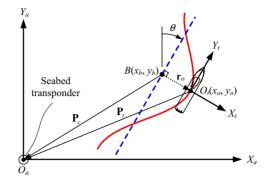$$Y_a = X_a \cot \theta + b \tag{2}$$

Figure 2. The vessel track and its linear fit are represented as a solid curve and a dashed line, respectively. The distance from point O_t to the reference course (dashed line) is the cross-track error.

where $\cot \theta$ is the slope of the reference course and b is the Y_a-intercept. The unit vector of the reference course with slope of $\cot \theta$ can be expressed as

$$e = \begin{bmatrix} \sin \theta \\ \cos \theta \\ 0 \end{bmatrix} \quad (3)$$

Let the coordinates of points O_t and B with respect to the global frame $O_a X_a Y_a Z_a$ be $(x_o, y_o, 0)$ and $(x_b, y_b, 0)$, respectively. Then, based on Equation (2), the distance vector from point B to point O_t is

$$\mathbf{r}_o^{(a)} = \begin{bmatrix} x_o - x_b \\ y_o - y_b \\ 0 \end{bmatrix} = \begin{bmatrix} x_o - x_b \\ y_o - x_b \cot \theta - b \\ 0 \end{bmatrix} \quad (4)$$

where the superscript a indicates that the vector $\mathbf{r}_o$ is with respect to the $O_a X_a Y_a Z_a$ frame. Because the distance vector $\mathbf{r}_o^{(a)}$ is perpendicular to the direction of the reference course, the coordinates of point B can therefore be obtained by solving the equation $\mathbf{e} \cdot \mathbf{r}_o^{(a)} = 0$ which gives

$$\begin{cases} x_b = (x_o \sin \theta + y_o \cos \theta) \sin \theta - b \sin \theta \cos \theta \\ y_b = (x_o \sin \theta + y_o \cos \theta) \cos \theta + b \sin^2 \theta \end{cases} \quad (5)$$

Substitute Equation (5) into Equation (4), the vector $\mathbf{r}_o^{(a)}$ becomes

$$\mathbf{r}_o^{(a)} = \begin{bmatrix} (x_o \cos \theta - y_o \sin \theta + b \sin \theta) \cos \theta \\ -(x_o \cos \theta - y_o \sin \theta + b \sin \theta) \sin \theta \\ 0 \end{bmatrix} \quad (6)$$

Since the USBL measurement $\mathbf{P}_t$ is relative to the $O_t X_t Y_t Z_t$ coordinate system, the correction for cross-track error has to be carried out in the same frame. Thus, the vector $\mathbf{r}_o^{(a)}$ is transformed into the $O_t X_t Y_t Z_t$ frame by applying the technique of
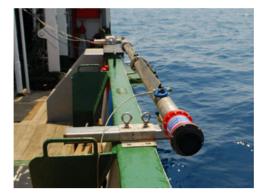
Figure 3. The USBL transceiver was installed on an over-the-side deployment pole.

coordinate transformation:

$$\mathbf{r}_o^{(t)} = \begin{bmatrix} \cos\theta & -\sin\theta & 0 \\ \sin\theta & \cos\theta & 0 \\ 0 & 0 & 1 \end{bmatrix} \mathbf{r}_o^{(a)} = \begin{bmatrix} x_o\cos\theta - y_o\sin\theta + b\sin\theta \\ 0 \\ 0 \end{bmatrix} \tag{7}$$

where the superscript t indicates that the vector $\mathbf{r}_o$ is with respect to the $O_t X_t Y_t Z_t$ frame. As illustrated in Figure 2, the corrected USBL measurement $\mathbf{P}_c$ can be obtained as

$$\boldsymbol{P}_c = \mathbf{r}_o^{(t)} + \boldsymbol{P}_t = \begin{bmatrix} P_{tx} + x_o\cos\theta - y_o\sin\theta + b\sin\theta \\ P_{ty} \\ P_{tz} \end{bmatrix} \tag{8}$$

where P_{tx}, P_{ty} and P_{tz} are the X_t, Y_t, and Z_t components, respectively, of the position vector $\mathbf{P}_t$.

4. FIELD EXPERIMENTAL RESULTS. The effectiveness and efficiency of the proposed algorithm for alignment error estimation is examined through a field experiment. The experiment was carried out with an off-the-shelf USBL positioning system in April 2010 off the coast of Kaohsiung Harbour, Taiwan. The USBL system has a positioning accuracy of $0\cdot25°$ (better than $0\cdot5\%$ of slant range.) Figure 3 shows the USBL transceiver that was mounted at the end of a pole and fixed on the side of the R/V Ocean Researcher III, a vessel operated by the National Sun Yat-sen University. The reference USBL transponder was mounted on the Seafloor Acoustic Transponder System (SATS) (Chen and Wang, 2011), as shown in Figure 4, and then deployed on the seabed at a water depth of about 300 m. In addition to the USBL positioning system, a Global Positioning System (GPS) and a gyrocompass with motion sensor were used to acquire data for the determinations of position and attitude of the USBL transceiver. The main characteristics of these instruments are summarized in Table 1.

Eight straight-line runs were carried out over the area above the seabed transponder to collect USBL observations and sensor data. The vessel tracks of the line survey are presented in Figure 5 and labeled L1-8. Sound-speed profiles of the water column were measured by taking conductivity-temperature-depth (CTD) casts over the period of

Table 1. The main sensors and instruments employed for the field experiment.

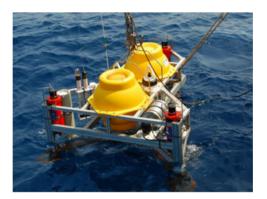| Sensor/Instrument	Accuracy
LinkQuest USBL Tracking system (TrackLink 1500HA)	Slant range: 20 cm Positioning: 0·25°
Trimble RTK GPS (5700 & 5800)	Horizontal: 1 cm ±1 ppm RMS Vertical: 2 cm ±1 ppm RMS
IXSEA OCTANS	Heading: 0·1° secant latitude Pitch: 0·01° RMS Roll: 0·01° RMS Heave: 5 cm

Figure 4. The Seafloor Acoustic Transponder System (SATS) was employed to carry and anchor reference USBL transponders to the seafloor.
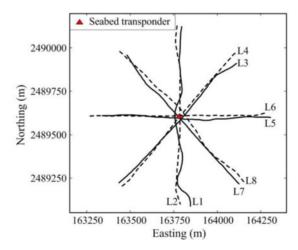

Figure 5. Vessel tracks L1-8 of the USBL line survey. The survey was centered on the reference seabed transponder that was at a depth of about 300 m.

line survey. Based on the collected observations of GPS and acoustic round-trip travel time with the combination of the given sound-speed profiles of the water column, the location of the seabed transponder was estimated by using the GPS/Acoustic
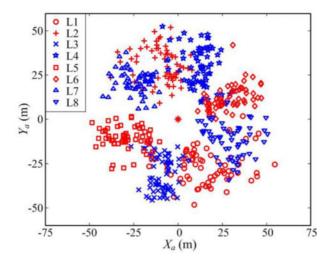
Figure 6. Seabed transponder positioning obtained directly from the raw USBL observations without misalignment correction. The asterisk is the location of the seabed transponder.

positioning technique (Chen and Wang, 2011). The estimates of the seabed transponder coordinates are given as $(P_{Tx}, P_{Ty}, P_{Tz}) = (163780 \cdot 57, 2489603 \cdot 35, -297 \cdot 09)$ m with respect to the Taiwan Datum 1997 (TWD97) 2-degree transverse Mercator (TM2), as shown in Figure 5. That is, the seabed transponder is at the depth of $297 \cdot 09$ m and the origin of the $O_a X_a Y_a Z_a$ frame is located at $(163780 \cdot 57, 2489603 \cdot 35, 0)$ m in the TWD97/TM2 coordinate system. Before the correction for alignment error is made, the USBL positioning of the seabed transponder with respect to the $O_a X_a Y_a Z_a$ coordinate system is presented in Figure 6, in which the data has been segregated by marker for the eight vessel tracks. As seen from Figure 6, the USBL positioning has errors distributed around the seabed transponder with standard deviations of $23 \cdot 4$, $25 \cdot 3$, and $27 \cdot 1$ m in the X_a-, Y_a-, and Z_a-directions, respectively. In addition, the scatter plot of the transponder positions is distributed with particular groupings related with individual survey paths.

4.1. *Corrections for heading deviation and cross-track error.* All of the transponder trajectories observed from the USBL transceiver are corrected for heading deviation and cross-track error before applying the proposed algorithm to estimate alignment errors. In the case of the transponder trajectory observed along the track L1, the vessel track with its linear fit is shown in Figure 7(a), the vessel's heading is in Figure 7(b), the cross-track error is in Figure 7(c), and the raw data of transponder trajectory observed along track L1 is in Figure 8(a). The slope of the linear fit to the vessel track L1 gives –37·25, corresponding to the reference course direction of $\theta = 358 \cdot 5°$. The heading deviation $\Delta\theta$ at any observation point is obtained as the difference between the measured vessel heading and the calculated reference direction. Then, by using Equation (1), the transponder positions are corrected for heading deviation, and the result is presented in Figure 8(b).

Having corrected for heading deviation, the transponder trajectory is further corrected for cross-track error by using Equation (8), and the result is shown in Figure 8(c). Figure 9 presents all the eight transponder trajectories before and after the corrections for heading deviation and cross-track error. It is clear from Figure 9 that
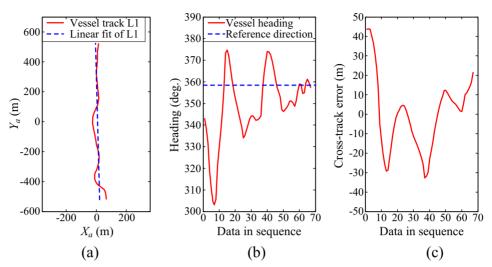
Figure 7. (a) Plot of the vessel track L1 and its linear fit in the $O_aX_aY_aZ_a$ coordinate system. (b) Heading of the vessel and the direction of the reference course derived from the linear fit of track L1. (c) Cross-track error of track L1.
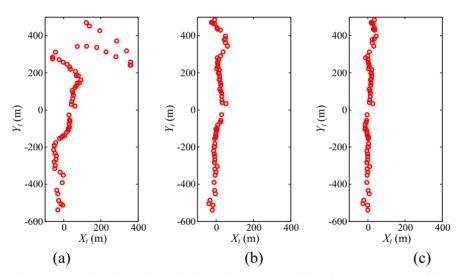

Figure 8. Corrections for heading deviation and cross-track deviation of the transponder positions observed along track L1. (a) Observed transponder positions. (b) Transponder positions after correction for heading deviation. (c) Transponder positions after corrections for heading deviation and cross-track error.

the corrections for heading deviation and cross-track error effectively reduce the distortion of the transponder trajectories, which in turn will result in a better estimation of alignment errors.

4.2. *Alignment error estimation.* Having corrected for heading deviation and cross-track error, the transponder trajectories are used to estimate the alignment errors. As indicated in Part I (Chen, 2013), the iterative process to estimate the
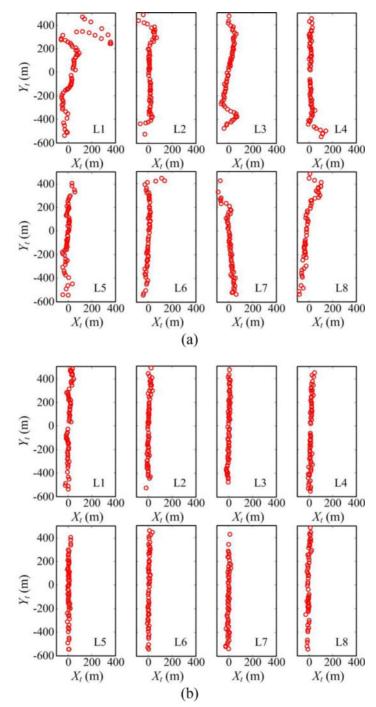
Figure 9. Transponder trajectories (a) before and (b) after the corrections for heading deviation and cross-track error.

alignment errors α, β, and γ with respect to heading, pitch and roll, respectively, is given by

$$\begin{cases} \alpha^{(k)} = \alpha^{(k-1)} + \Delta\alpha \\ \beta^{(k)} = \beta^{(k-1)} + \Delta\beta, \quad k = 1, \ 2, \ 3, \cdots \\ \gamma^{(k)} = \gamma^{(k-1)} + \Delta\gamma \end{cases} \tag{9}$$

where k is the iteration number, and $\Delta\alpha$, $\Delta\beta$, and $\Delta\gamma$ are increments of estimates. At each iteration, the increments $\Delta\alpha$ and $\Delta\beta$ are computed by

$$\Delta\alpha = \cot^{-1}(m_{xy}) \tag{10}$$

$$\Delta\beta = -\tan^{-1}(m_{yz}) \tag{11}$$

where m_{xy} and m_{yz} are the slopes of transponder trajectory on X_t-Y_t and Y_t-Z_t planes, respectively. As for the increment $\Delta\gamma$ of roll alignment error, it can be solved from either of the following two equations:

$$X_t = -d\cos\Delta\gamma - P_{Tz}\sin\Delta\gamma \tag{12}$$

$$Z_t = -d\sin\Delta\gamma + P_{Tz}\cos\Delta\gamma \tag{13}$$

where d is the horizontal distance from the seabed transponder to the vessel track and $-P_{Tz}$ represents the depth of the seabed transponder (i.e., $P_{Tz} = -297 \cdot 09$ m).

Here we take the positioning data collected along track L1 as an example to illustrate the numerical estimation of alignment errors at the first iteration.

4.2.1 *Heading misalignment estimation.* Figure 10(a) presents the positioning data that has been corrected for heading deviation and cross-track error. It should be noted that the aspect ratio of the plots in Figure 10 is not equal to one for better interpretation of slope of the transponder trajectory. All iterative methods require that initial guesses be provided for each parameter. In all cases the initial guesses were taken to be the constant 0 (i.e., $\alpha^{(0)} = \beta^{(0)} = \gamma^{(0)} = 0$) for iteration zero ($k = 0$). The positioning data in Figure 10(a) is fitted to a straight line by linear regression, which is shown as the solid line. The slope of the fitted line on the X_t-Y_t plane is $m_{xy} = 27 \cdot 65$ corresponding to heading alignment error $\alpha = 2 \cdot 07°$. The transponder trajectory is then corrected for the estimate $\alpha = 2 \cdot 07°$ and the result is shown in Figure 10(b), in which the fitted line of the transponder trajectory on the X_t-Y_t plane becomes much steeper and its slope increases to $1 \cdot 5E4$.

4.2.2 *Pitch misalignment estimation.* The pitch alignment error is determined based on the slope of the transponder trajectory on the Y_t-Z_t plane. In Figure 10(b), the transponder trajectory on the Y_t-Z_t plane is fitted to a straight line which has a slope of $-0 \cdot 079$. Substituting $m_{yz} = -0 \cdot 079$ into Equation (11) yields $\beta = 4 \cdot 52°$. The transponder trajectory corrected for the estimates $\alpha = 2 \cdot 07°$ and $\beta = 4 \cdot 52°$ is presented in Figure 10(c), in which the linear fit of the trajectory on the Y_t-Z_t plane becomes flatter and its slope is improved from $-0 \cdot 079$ to $-0 \cdot 007$.

4.2.3 *Roll misalignment estimation.* In this case, we use Equation (12) to solve for the roll alignment error. The relevant parameters in Equation (12) include X_t, d, and P_{Tz}. As can be seen from Figure 10(c), the X_t coordinates of the positioning data are not identical. The value of the parameter X_t is therefore given by the average of the X_t coordinates of the transponder trajectory, which yields $X_t = 2.15$ m. For the parameter d, it is defined as the horizontal distance from the seabed transponder to the vessel track (L1 in this case). Because the track L1 is non-straight and its linear fit is
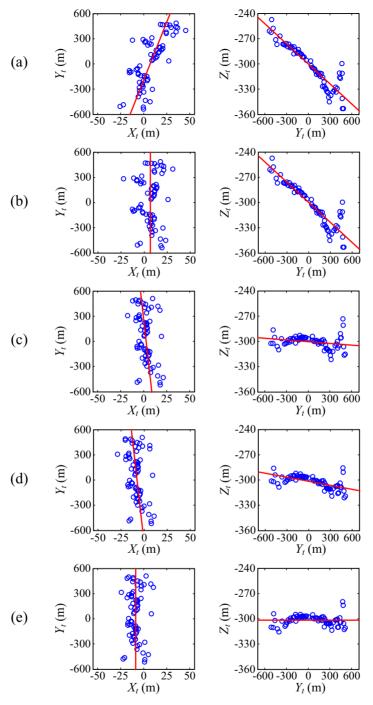
Figure 10. Iterative alignment error correction of the positioning data collected along track L1. The circle and the solid line represent the positioning data and its linear fit, respectively. (a) Initial data without alignment error correction. (b) Result with correction for $\alpha = 2{\cdot}07°$. (c) Result with correction for $\alpha = 2{\cdot}07°$ and $\beta = 4.52°$. (d) Result with correction for $\alpha = 2{\cdot}07°$, $\beta = 4.52°$, and $\gamma = 2.09°$. (e) After 5 iterations.

Table 2. Iteration history for alignment error estimation with positioning data collected along track L1.

Iteration number (k)	Estimates of alignment errors (degree)					
	$\Delta\alpha$	$\Delta\beta$	$\Delta\gamma$	α	β	γ
0				0	0	0
1	2·0714	4·5184	2·0853	2·0714	4·5184	2·0853
2	− 0·5864	0·9096	0·0230	1·4850	5·4280	2·1083
3	− 0·1168	0·0751	0·0077	1·3682	5·5031	2·1160
4	− 0·0097	0·0076	0·0007	1·3585	5·5107	2·1167
5	− 0·0009	0·0007	0·0000	1·3576	5·5114	2·1167
6	− 0·0002	0·0001	0·0000	1·3574	5·5115	2·1167

Table 3. Estimates of alignment errors as obtained from different positioning data collected along tracks L1-8. Note that the roll alignment error, γ, is obtained by Equation (12).

Vessel Track	Estimates of alignment errors (degree)			No. of iterations*
	α	β	γ	
L1	1·3575	5·5114	2·1167	5
L2	1·1604	5·7456	1·8131	4
L3	0·8578	5·9504	2·0139	4
L4	1·2423	5·6839	2·0486	4
L5	0·5105	5·5824	2·0703	4
L6	0·8156	5·2762	2·0409	4
L7	0·8891	6·0809	1·5262	4
L8	1·0934	5·4294	2·1278	4
Mean	0·9908	5·6575	1·9697	
Standard deviation	0·2742	0·2667	0·2040	

* The iteration is terminated when all estimates of α, β, and γ have converged to within 0·001 degrees.

used as reference for the correction of cross-track error, the value of d is thereby the horizontal distance from the transponder to the linear fit of track L1, which yields $d = 8\cdot67$ m. Substituting $P_{Tz} = -297\cdot09$, $X_t = 2.15$, and $d = 8\cdot67$ into Equation (12), we obtain the roll alignment error as $\gamma = 2\cdot09°$. The transponder trajectory corrected for the estimates $\alpha = 2\cdot07°$, $\beta = 4\cdot52°$ and $\gamma = 2\cdot09°$ is presented in Figure 10(d).

The iterative process is repeated until all estimates of three alignment errors have converged to some tolerance. Table 2 gives the history of the estimates of three alignment errors as generated by the iterative procedure. As can be seen, all estimates of α, β, and γ have converged to within 0·001 degrees after five iterations, yielding the final estimates $\alpha = 1\cdot36°$, $\beta = 5\cdot51°$, and $\gamma = 2\cdot12°$. The estimation demonstrates that the rate of convergence of the algorithm is quite fast in practice. Figure 10(e) shows the corrected transponder trajectory after 5 iterations, in which the slope m_{xy} is −6·07E5 and the slope m_{yz} is −1·25E − 6. As expected, on completion of alignment error correction, the magnitudes of the slopes m_{xy} and m_{yz} are close to infinity and zero, respectively.

The algorithm is further tested on the positioning data collected along tracks L2-8. Table 3 summaries the final results of alignment error estimation with each dataset collected along different tracks. Note that all the estimates of roll alignment error
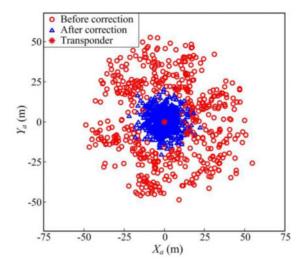
Figure 11. Position of the seabed transponder as measured with and without the correction for alignment errors, in which the estimates of roll alignment error is based on Equation (12).

given in Table 3 are obtained by Equation (12). In the estimation of alignment errors, our termination criterion is to stop the iteration if the increments $\Delta\alpha$, $\Delta\beta$, and $\Delta\gamma$ are all less than 0·001 degrees. As can be seen from Table 3, convergence is very fast and is obtained in five iterations for all eight cases, indicating high efficiency of the proposed algorithm in the estimation of alignment errors. In the bottom two rows of Table 3 the mean and standard deviation are given, respectively, of the estimates obtained from the eight cases. The standard deviations of the estimates for different data sets are small (within 0·3 degrees), which indicates the alignment errors are robustly estimated from the positioning data. The correction for transceiver alignment error is done by the use of the mean estimates listed in Table 3 and the USBL positioning result is presented in Figure 11. As is seen, the corrected positioning data forms a concentrated point cloud around the true location of the transponder. After misalignment calibration, the error standard deviations of the USBL positioning are significantly reduced from 23·4, 25·3, and 27·1 m to 7·3, 7·0, and 5·9 m in the X_a-, Y_a-, and Z_a-directions, respectively.

4.3. Estimation of roll alignment error. As mentioned earlier, the determination of roll alignment error in the proposed algorithm can be carried out by solving either Equation (12) or Equation (13). That is, the roll alignment error has a coordinate dependence and can be given in terms of either X_t or Z_t:

$$\gamma = \gamma^{(x)}(X_t, d, P_{Tz}) = \gamma^{(z)}(Z_t, d, P_{Tz}) \tag{14}$$

In Part I (Chen, 2013), we have shown that $\gamma^{(x)}$ is more robust to the noise in USBL measurements than $\gamma^{(z)}$ in the determination of roll alignment error when the condition $|d| < |P_{Tz}|$ is true. In this subsection, we aimed to verify this finding with the use of data from observations of USBL positioning.

Table 4 shows the horizontal distance d from the seabed transponder to each of the eight vessel tracks. It can be observed from Table 4 that the distances, $|d|$, to the vessel tracks are all much less than the depth of the seabed transponder (297·09 m),

Table 4. Estimates of alignment errors as obtained from different positioning data collected along tracks L1-8. Note that the roll alignment error, γ, is obtained by Equation (13).

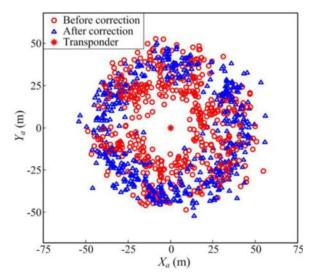| Vessel Track	d (m)	Estimates of alignment errors (degree)		
		α	β	$\gamma^{(z)}$
L1	8·67	0·1096	9·8339	18·3606
L2	3·71	0·4212	5·7980	12·9649
L3	13·03	0·0600	6·4025	12·5117
L4	− 7·56	1·7901	6·0736	− 6·1898
L5	5·38	0·0469	5·9110	9·3590
L6	5·33	0·2443	5·7694	11·6286
L7	4·25	0·4314	5·1987	9·0302
L8	16·99	0·7044	6·2735	7·8410
Mean		0·4760	6·4076	9·4383
Standard deviation		0·5768	1·4321	7·1038

Figure 12. Position of the seabed transponder as measured with and without the correction for alignment errors, in which the estimates of roll alignment error is based on Equation (13).

i.e., $|d| \ll |P_{Tz}|$. Therefore, $\gamma^{(z)}$ is expected to be much more sensitive to measurement noise than $\gamma^{(x)}$. By solving γ from Equation (13), the estimates of alignment errors with each dataset collected along different tracks are obtained and listed in Table 4. Apparently, the standard deviation of the estimates of $\gamma^{(z)}$ in Table 4 is much higher than that of $\gamma^{(x)}$ in Table 3, which is in agreement with our findings in Part I (Chen, 2013). Moreover, imprecise estimation of roll alignment error increases the variance in the estimates of heading and pitch alignment errors as well.

By the use of the mean estimates listed in Table 4, the transponder positioning is corrected for the alignment errors of $\alpha = 0.48°$, $\beta = 6.41°$, and $\gamma = 9.44°$ and the result is presented in Figure 12. It is clear by comparing Figure 12 with Figure 11 that the estimates of alignment errors in Table 4 are quite unreliable and no improvement is made on the accuracy of transponder positioning. A robust estimation of roll

alignment error is therefore crucial in achieving effective misalignment calibration of a USBL navigation system.

5. CONCLUSION. The proposed algorithm for Ultra Short Baseline (USBL) alignment calibration has been tested using the data collected from a field experiment. Effective solutions have been provided to correct the effects of vessel's heading deviation and cross-track error on the estimation of alignment errors. Therefore, with the aids of heading deviation and cross-track error corrections, the vessel trajectory for USBL calibration is not limited to a straight line but can be any arbitrary curve. Similar to the simulation results in Part I (Chen, 2013), the filed experimental results show that the proposed algorithm has a fast convergence speed. For the eight USBL line surveys conducted, all the estimates of alignment errors have converged to within a tolerance of 0·001 degrees in five iterations. Furthermore, the variance of the estimates obtained from the eight USBL line surveys is small, indicating the robustness of the proposed algorithm on the estimation of alignment errors.

On the estimation of roll alignment error, the experimental results agree well with the theoretical predictions derived in Part I. It is shown that, when the horizontal distance from the seabed transponder to the vessel track is less than the depth of the transponder, $\gamma^{(x)}$ (estimation using X_t-coordinate data of USBL positioning) is more robust than $\gamma^{(z)}$ (estimation using Z_t-coordinate data of USBL positioning) in the determination of roll alignment error. In particular, by the use of $\gamma^{(z)}$, the variance of the estimate of roll alignment error increases significantly as the horizontal distance from the seabed transponder to the vessel track is close to zero. The experimental results also show that as the variance of the estimate of roll alignment error increases, so do the estimates of heading and pitch alignment errors.

REFERENCES

Chen, H. H. (2013). The Estimation of Angular Misalignments for Ultra Short Baseline Navigation Systems. Part I: Numerical Simulations. *The Journal of Navigation*, **66(3)**.

Chen, H. H. and Wang, C. C. (2011). Accuracy Assessment of GPS/Acoustic Positioning Using a Seafloor Acoustic Transponder System. *Ocean Engineering*, **38(13)**, 1472–1479.

Gierusz, W., Cong Vinh, N. and Rak, A. (2007). Maneuvering Control and Trajectory Tracking of Very Large Crude Carrier. *Ocean Engineering*, **34 (7)**, 932–945.

Moreira, L., Fossen, T. I. and Guedes Soares, C. (2007). Path Following Control System for a Tanker Ship Model. *Ocean Engineering*, **34 (14)**, 2074–2085.

Skjetne, R., Fossen, T. I. and Kokotović, P. V. (2005). Adaptive Maneuvering, with Experiments, for a Model Ship in a Marine Control Laboratory. *Automatica*, **41(2)**, 289–298.